
Structural Analysis of Leukotriene C₄ Isomers Using Collisional Activation and 157 nm Photodissociation

Arugadoss Devakumar,^a David K. O'Dell,^b J. Michael Walker,^b and James P. Reilly^a

^a Department of Chemistry, Indiana University, Bloomington, Indiana, USA

^b Gill Center for Biomolecular Science, Indiana University, Bloomington, Indiana, USA

The fragmentation of 5-hydroxy-6-glutathionyl-7,9,11,14-eicosatetraenoic acid [leukotriene C₄ or LTC₄ (5, 6)] and its isomeric counterpart LTC₄ (14, 15) were studied by low and high-energy collisional induced dissociation (CID) and 157 nm photofragmentation. For singly charged protonated LTC₄ precursors, photodissociation significantly enhances the signal intensities of informative fragment ions that are very important to distinguish the two LTC₄ isomers and generates a few additional fragment ions that are not usually observed in CID experiments. The ion trap enables MSⁿ experiments on the fragment ions generated by photodissociation. Photofragmentation is found to be suitable for the structural identification and isomeric differentiation of cysteinyl leukotrienes and is more informative than low or high-energy CID. We describe for the first time the structural characterization of the LTC₄ (14, 15) isomer by mass spectrometry using CID and 157 nm light activation methods. (J Am Soc Mass Spectrom 2008, 19, 14–26) © 2008 American Society for Mass Spectrometry

Eicosanoids are oxygenated metabolites of polyunsaturated fatty acids, mainly arachidonic acid with 20 carbon atoms. Prostaglandins, thromboxanes, leukotrienes, and other hydroxy and epoxy fatty acids belong to this diverse family of biologically active metabolites. They are enzymatically formed by cyclooxygenase or by specific lipoxygenases and epoxygenases [1–4]. Their role in a broad range of diseases, such as atherosclerosis, immunologic-allergic reactions, and inflammatory disorders, is widely acknowledged [2, 5–7]. These molecules are synthesized within cells in response to various stimuli. Following their release, they interact with specific G-protein coupled receptors [4, 5]. Thus, these molecules serve an important role as chemical communicators of cellular activation. Among the various products of the lipoxygenase (LOX) pathway of arachidonic acid metabolism, the class of compounds called “slow reacting substance of anaphylaxis” (SRS-A) has received the most attention because of their potent biological activities [5]. SRS-A consists of varying amounts of the cysteinyl leukotrienes LTC₄, LTD₄, and LTE₄, all derived from a common biological precursor LTA₄. The leukotrienes are derived from the 5-lipoxygenase pathway of metabolism typically by inflammatory cells such as eosinophils, monocytes, macrophages, and mast cells [5, 8, 9]. 5-Lipoxygenase activating protein sequentially converts arachidonic acid into 5-hydroperoxyeicosatetraenoic acid (5-HPETE), and

then 5-HPETE into the reactive allylic epoxide leukotriene called A₄ (LTA₄). The 5-hydroxy-6-glutathionyl-7,9,11,14-eicosatetraenoic acid named LTC₄ can be produced by the conjugation of LTA₄ with tripeptide glutathione in the presence of leukotriene C₄ synthases [6]. Other members of the SRS-A family include LTD₄ and LTE₄ corresponding to the cysteinyl glycine and cysteine adducts of LTA₄. LTC₄ catabolism involves peptide cleavage reactions involving glutamyl transpeptidase and various dipeptidases to yield LTD₄ and LTE₄, both of which have biological activity. The cell can chemically transform LTA₄ into LTB₄ depending on the presence of A₄ hydrolases. LTC₄, LTD₄, and LTE₄ are collectively referred to as cysteinyl leukotrienes.

Cysteinyl leukotrienes provoke contractions of various smooth muscles and have been implicated as mediators of acute hypersensitivity reactions including asthma [2]. The involvement of cysteinyl leukotrienes in bronchial asthma has been clinically demonstrated [10]. There is great interest currently in drugs that inhibit the leukotriene-dependent bronchial contraction and reduce the intensity of bronchial spasms [1]. Mass spectrometry has been widely used to elucidate the role and structure of cysteinyl-leukotrienes for almost two decades. The first direct analysis of intact native cysteinyl leukotrienes was accomplished using fast atom bombardment ionization (FAB) mass spectrometry by Murphy and coworkers [11]. Both positive and negative ion FAB spectra of cysteinyl leukotrienes show intense molecular ions and weak fragment ions due to the loss of the cysteine-containing moiety. Although FAB pro-

Address reprint requests to Dr. J. P. Reilly, Department of Chemistry, Indiana University, Bloomington, IN 47405, USA. E-mail: reilly@indiana.edu

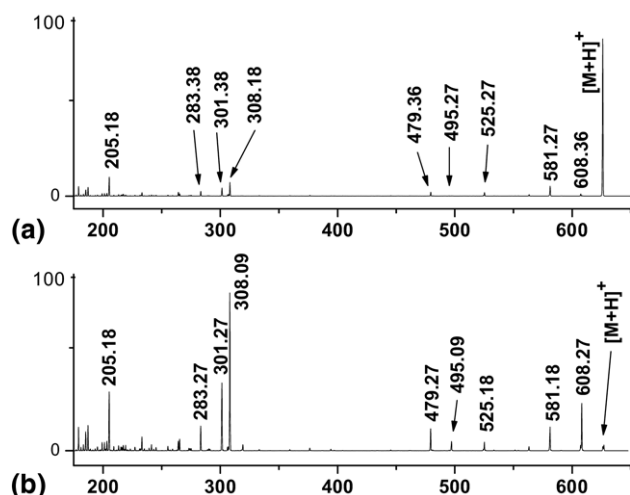
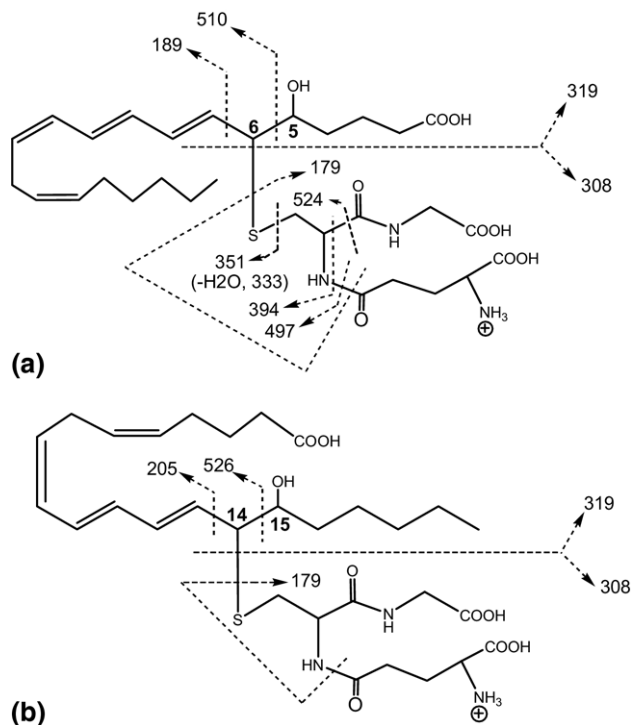


Figure 1. MS² spectra of singly charged protonated LTC₄ (14, 15) isomer [M + H]⁺ (precursor ion: *m/z* 626) (a) 157 nm photodissociation in ion trap, (b) combination of 157 nm light and CID (using 15% normalized collisional energy).

vides information on the molecular ion, the mass spectra contain little structural information. The introduction of matrix-assisted laser desorption-ionization (MALDI) mass spectrometry dramatically changed the status of biomolecular analysis. The simple addition of matrix to the sample preparation provides soft and efficient ionization of various fragile, nonvolatile samples. Despite its advantages, MALDI has not been extensively used for the characterization of low molecular weight compounds. In MALDI mass spectrometric analysis, the alkali metal ions in the sample promote the formation of matrix clusters and their alkali ion adducts, suppressing the analyte signals, particularly in the low mass region [12, 13]. As an alternative, electrospray ionization (ESI) has become the ionization method of choice to eliminate matrix chemical noise [14]. More recently, ESI tandem mass spectrometry of eicosanoids has been reviewed by Murphy et al. [15]. Collisions of both positive and negative molecular ion species ([M + H]⁺ and [M - H]⁻) with neutral atoms at low-pressure can drive unique rearrangement reactions and break carbon-carbon bonds to generate abundant ion products. While mass spectrometric studies to define the chemical structure of leukotrienes have been performed, identifying and distinguishing structurally related isomers and isobaric eicosanoids remains challenging. Deuterated derivatives of LTC₄ and the structurally related 5-oxo-7-gluthathionyl-8,11,14-eicosatrienoic acid (FOG₇) have been distinguished by MS³ tandem mass spectrometry [16]. The mammalian lipoxygenase enzymes produce 5-, 12-, and 15-hydroperoxides that can in turn give rise to numerous structurally related compounds. Distinguishing these similar molecules is a challenging task and new methods to accomplish this would be very helpful. Little is known about the existence of other cysteinyl leukotrienes arising from either alternative LOX metabolism (12 or 15) or similar compounds arising from glutathione ring opening of epoxides produced by

epoxygenase metabolism [17–19]. The biological significance of leukotriene-14, 15 analogs presented by Reddanna et al. and Sala et al. leads to an increasing need to characterize the structures of these compounds [17, 19].

We recently reported that 157 nm laser photodissociation of peptide ions generates high-energy backbone and side-chain cleavages [20–22]. Singly charged peptides having C- or N-terminal arginine residues were found to preferentially fragment between their α- and carbonyl-carbon atoms, yielding rather uniform and easily interpretable distributions of x- and a-type ions. On the basis of previous spectroscopic studies we proposed that the chromophore involved in this process is the backbone amide. Carbohydrate photofragmentation has also been reported recently by our group [23, 24]. We have shown that the photodissociation yielded intense cross-ring fragmentations for Girard's T derivatized oligosaccharides and the product ions are similar to those observed in high-energy CID experiments. Unfortunately, there is no spectroscopic or photochemical information on leukotrienes in the vacuum ultraviolet (VUV) or infrared (IR) regions. Fundamental studies are required to fully understand the leukotrienes photofragmentation mechanism. Herein we report the first investigation of leukotriene photodissociation and its applicability for distinguishing regioisomers. In the present work, the LTC₄ (5, 6) and (14, 15) isomers are photofragmented using 157 nm light in an ion trap, and the results are compared with high- and low-energy CID data. Our results suggest that the product ions generated by photodissociation of these molecules were corresponding to high-energy CID pathway.



Scheme 1. Structures and assignments of the fragments observed for (a) LTC₄ (5, 6) isomer, (b) LTC₄ (14, 15) isomer.

Experimental

Materials

Sodium chloride and α -cyano-4-hydroxycinnamic acid (CHCA) was obtained from Sigma-Aldrich (St. Louis, MO), methanol was purchased from EMD (Gibbstown, NJ), and Glacial acetic acid was obtained from Mallinckrodt (Phillipsburg, NJ). Leukotriene- C_4 (LTC_4) (5, 6) isomer was purchased from Cayman Chemical Company (Ann Arbor, MI) and LTC_4 (14, 15) isomer

was supplied by BIOMOL Research Laboratories (Plymouth meeting, PA). All water used in these experiments was purified by an E-pure water filtration system from Barnstead Thermolyne Co. (Dubuque, IA).

Mass Spectrometry

Electrospray experiments were performed on a Finnigan LTQ mass spectrometer (Thermo Electron, San Jose, CA) equipped with an ESI source. All samples were

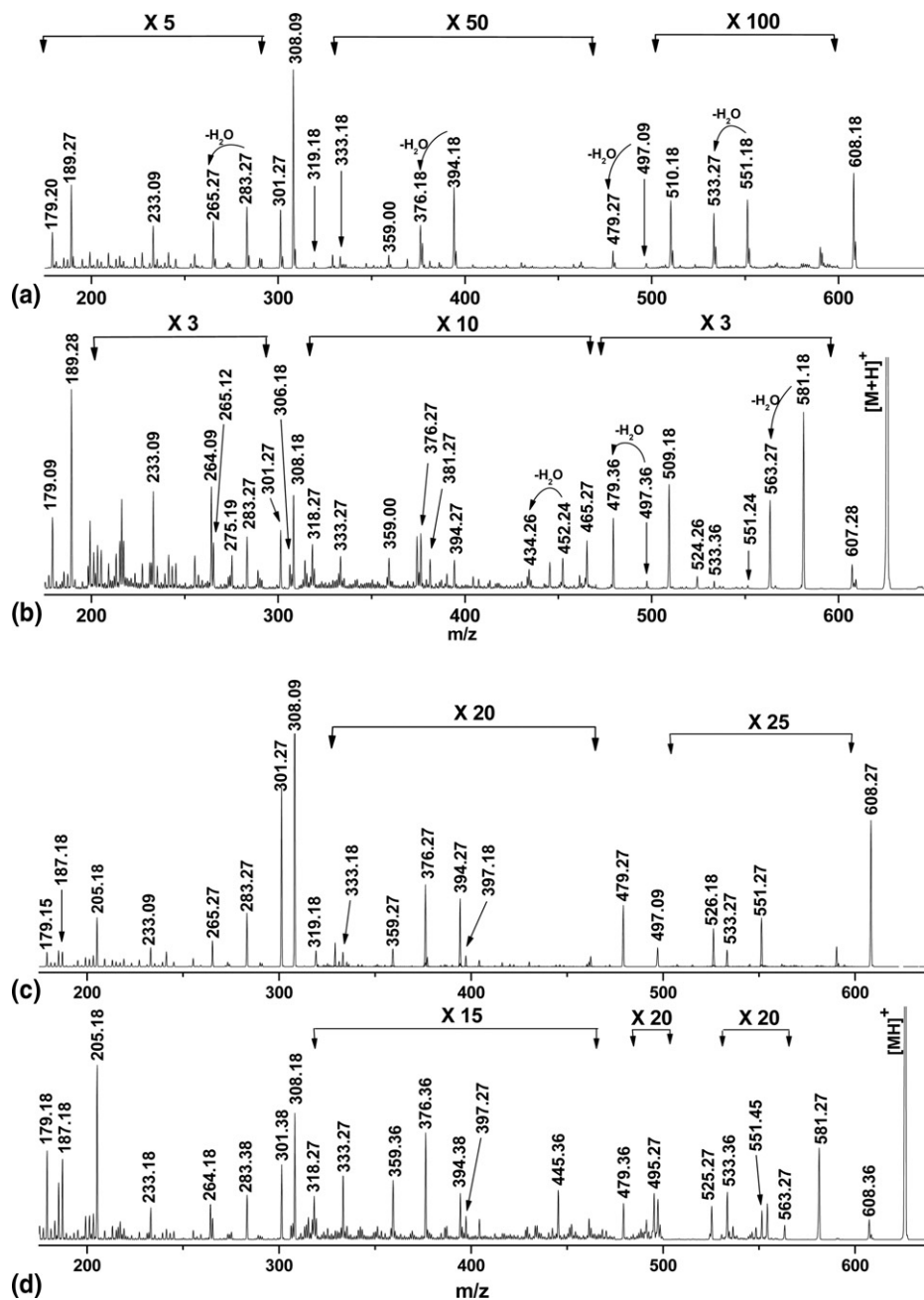


Figure 2. MS^2 spectra of $[M + H]^+ LTC_4$ (5, 6) isomer obtained by (a) low-energy CID in linear ion trap, (b) 157 nm photodissociation in ion trap. MS^2 spectra of $[M + H]^+ LTC_4$ (14, 15) isomer obtained by (c) low-energy CID in linear ion trap, (d) 157 nm photodissociation in ion trap. Note changes in vertical scale within the spectrum.

infused into the mass spectrometer at a flow rate of 3 $\mu\text{L}/\text{min}$ by a syringe pump. For protonated LTC₄ experiments the sample solutions ($\sim 10 \mu\text{M}$ concentrations) were prepared in 1:1 MeOH/H₂O with 2% acetic acid; 2 mM sodium chloride was added to this for sodium cationized LTC₄ experiments to improve the precursor ion signal. The ion injection time was set to 300–1000 ms with an isolation width of 1 Da to select precursor ions. CID of precursor ions was accomplished by applying a resonant RF excitation waveform for 30 ms with activation Q of 0.25. Normalized collision energy of 35% to 50% was used and spectra are the average of 60 micro scans. The LTQ was slightly modified to be compatible with 157 nm photodissociation [21, 23, 24]. Briefly, an F₂ laser (EX100HF-60; GAM Laser, Orlando, FL), producing 2 mJ of light in a 10 ns pulse, was connected to the back of the LTQ instrument with a vacuum line. The unfocused light was introduced through a 1.7 mm diameter aperture aligned with the preexisting 2 mm hole in the back lens of the ion trap. Based on the size of the aperture and the laser beam profile, we estimate that about 40 μJ of light pass through the ion trap. After irradiating the trapped ions, most of the light then exits through the hole in the front

lens of the trap. The precursor ion isolation conditions for MS² photodissociation experiments were the same as in CID, except that the normalized collision energy was set to 0%. The laser was triggered by the LTQ at the beginning of the activation stage. To pursue MS³ experiments, the signal intensities of MS² fragment ions need to be improved. This can be achieved by conducting hybrid MS² CID experiments, where 5% to 15% of normalized collision energy was combined with 157 nm light. This process of activation significantly improves the signal intensities of MS² photofragments. Once an ion of interest is selected for MS³ experiments, 25% to 35% of normalized collision energy was used for further fragmentation.

An Applied Biosystems (Foster City, CA) 4800 proteomics analyzer was utilized for high-energy 1 keV CID experiments with argon collision gas at a pressure of 5×10^{-7} torr. The precursor ion selection window was set at 5 Da. MALDI spots for LTC₄ isomers were prepared by dissolving ~ 20 pmol of the dried samples in 10 μL of CHCA matrix solution (10 g/L) in 1:1 vol/vol acetonitrile/water containing 0.1% TFA. For sodium cationized experiments, water containing 2 mM sodium chloride was used in matrix preparation.

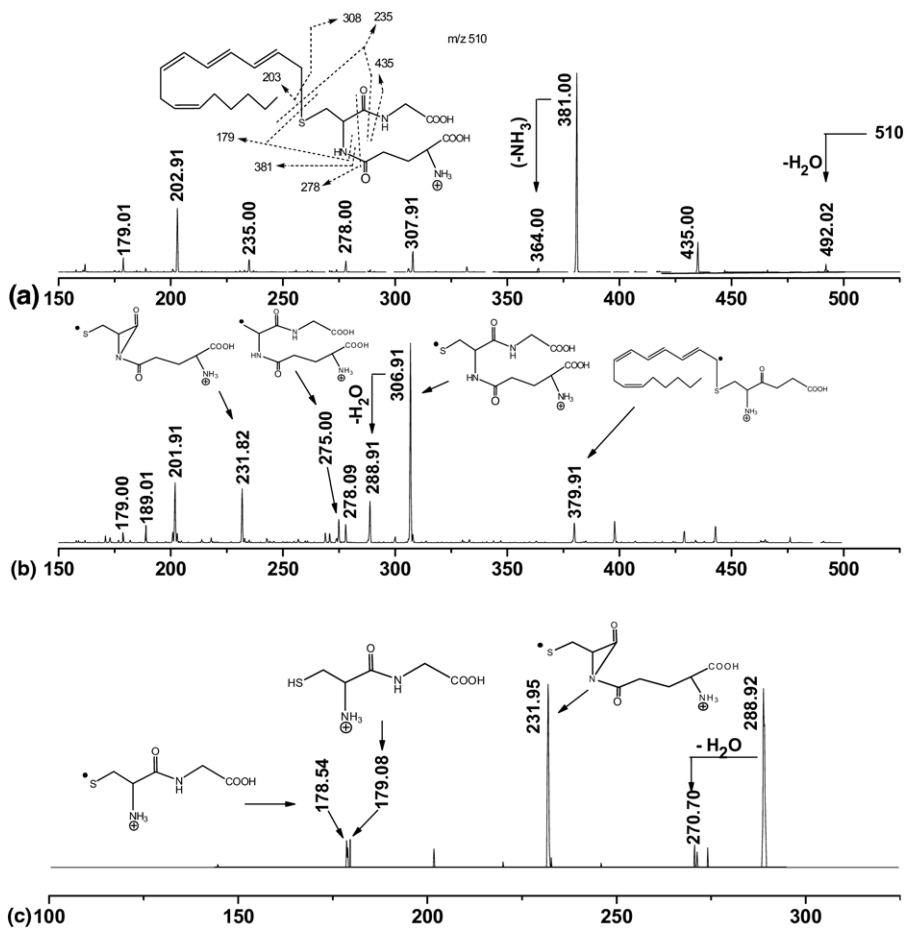


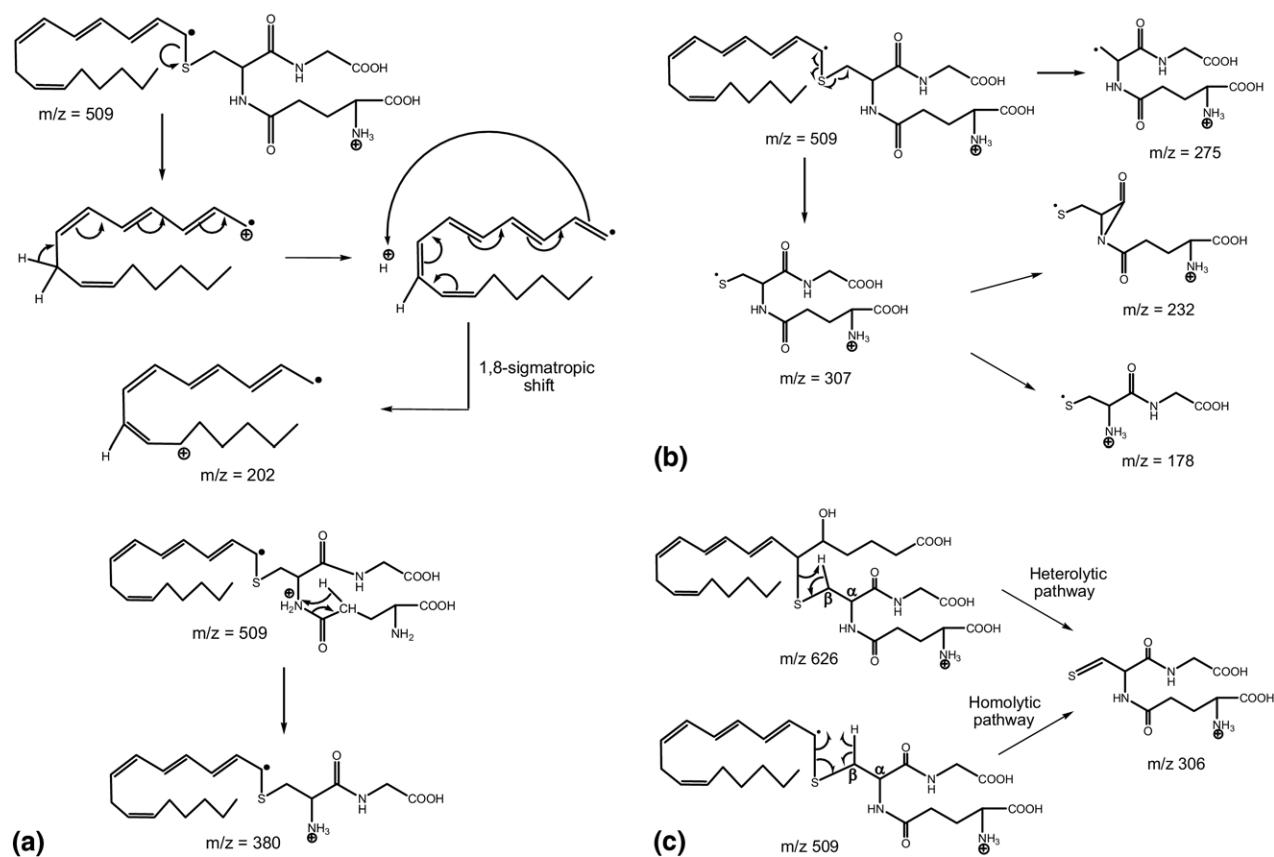
Figure 3. (a) MS³ CID spectrum of the fragment m/z 510 obtained from LTC₄ (5, 6) collisional activation, (b) MS³ CID spectrum of the photofragment m/z 509 obtained from LTC₄ (5, 6), (c) MS⁴ CID spectrum of fragment m/z 307 obtained by hybrid MS³ experiment.

Results and Discussion

Scheme 1 displays the structures of LTC₄ isomers (5, 6) and (14, 15). In the (5, 6) isomer the hydroxyl group is attached to carbon-5 and the tripeptide unit consisting of cysteine-glycine-glutamic acid is bonded to lipid backbone carbon-6 via a thio-ether bond. The (14, 15) isomer contains the tripeptide unit at carbon-14 and the hydroxyl group at carbon-15. The positional isomers can be distinguished through the formation of specific fragment ions. Examples are *m/z* 189 (obtained by C6–C7 bond cleavage on lipid backbone) or 510 (cleavage of C5–C6 bond on lipid backbone) for the (5, 6) isomer and *m/z* 205 (cleavage of C13–C14 bond on lipid backbone) or 525 (cleavage of C14–C15 bond on lipid backbone) for the (14, 15) isomer. Any tandem MS analysis that produces these characteristic fragment ions can successfully differentiate these two isomers. Scheme 1 presents the notation where the charge is tentatively assigned on the most basic site of the molecule. However, in certain cases, the nonbasic lipid chain can also retain the charge during collisional activation as shown by Hevko and Murphy [16]. For instance, the fragment ion *m/z* 189 mentioned above is a resonance stabilized alkyl cation, where the charge resides on the carbon chain of the lipid molecule. It has been shown to

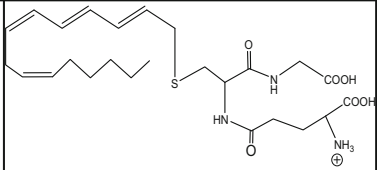
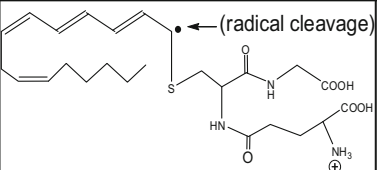
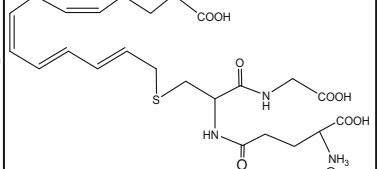
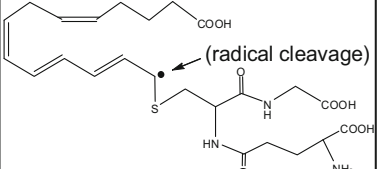
arise from a protonated epoxide cation through a step-wise rearrangement mechanism involving heterolytic bond cleavages [16]. In this report, we specifically focus on photofragmentation results that are different from those obtained with CID experiments.

As we reported in our earlier 157 nm photofragmentation experiments, with the current experimental configuration precursor depletion rates of ~25% have been obtained [22, 23]. In some cases, dozens of different fragment ions form from a single precursor, and this significantly limits the intensity of each one. However, this may not be an insurmountable problem since the light intensity and the number of trapped ions can be increased, and we are able to perform hybrid MS³ experiments. To increase the fragmentation efficiency, we tried applying some collisional energy during a 157 nm photofragmentation experiment. Figure 1a shows the MS² mass spectrum of singly charged protonated LTC₄ (14, 15) obtained with 157 nm photodissociation alone. The MS² spectrum shown in Figure 1b was recorded by combining 15% of normalized collision energy with 157 nm light. It is evident that adding collisional excitation does not change the types of photofragments formed but simply improves the MSⁿ signal. This approach was used throughout this work to



Scheme 2. Generation of radical product ions from the radical precursor ion *m/z* 509 (a) *m/z* 202 and 380 via heterolytic bond cleavage, (b) *m/z* 178, 232, 275, and 307 via homolytic bond cleavage, (c) proposed pathway for the formation ion *m/z* 306 from *m/z* 626 and 509.

Table 1. Key product ions generated during CID and photofragmentation of LTC₄ isomers

LTC ₄	CID fragment			157 nm Photofragment		
		Monoisotopic Mass	Observed Mass		Monoisotopic Mass	Observed Mass
(5, 6) Isomer		510.26	510.18		509.26	509.18
(14, 15) Isomer		526.22	526.18		525.21	525.27

obtain MSⁿ where $n > 2$. This process yielded cleaner spectra with better signal-to-noise.

Protonated LTC₄ (5, 6) Isomer

The low-energy CID spectrum displayed in Figure 2a was generated in the linear ion trap instrument from protonated LTC₄ (5, 6) isomer with singly-charged precursor m/z 626 in positive ion mode. The ions observed are similar to those previously reported for the CID of [M + H]⁺ ions of LTC₄ (5, 6) namely, m/z 179, 189, 265, 283, 308, 319, 497, 510, and 608 [14, 16, 25]. Scheme 1a shows the fragmentation pattern of these familiar ions. Fragments m/z 189 and 510 are the two most important features distinguishing the (5, 6) and (14, 15) isomers. Although the peak at m/z 189 appeared weaker than other fragments in the spectrum, its signal was sufficient to perform MS³ experiments. Results confirmed that the m/z 189 ion is the product of C6-C7 lipid backbone cleavage whose mechanism of formation was previously reported by Murphy and coworkers [16]. The structure of the other weak diagnostic ion m/z 510 has not been previously characterized by MS³ CID experiments. It was possible, however, to obtain a CID spectrum of this ion by infusing a higher (~20 μM) sample concentration. The result is presented in Figure 3a with an inset illustrating the assignments of the observed fragments. The spectrum displays an interesting series of fragment ions at m/z 179, 203, 235, 278, 308, 364, 381, 435, and 492. At this stage, four features that help to determine the partial lipid backbone structure in m/z 510 were observed. The most intense peak at m/z 381 was formed by cleavage of the peptide bond between cysteine and glutamate amino acids as depicted in the spectrum inset. A minor feature at m/z 364, likely a result of the loss of ammonia from m/z 381, was also observed. Cleavage of the peptide bond between cysteine and glycine yielded the product ion m/z 435.

Cleavage of the C6-S bond with charge retention on the partial lipid chain produced a resonance stabilized allylic cation m/z 203. The fourth distinct feature at m/z 278 was formed by two cleavages: the cysteine-glutamate peptide bond and the bond between C α and the carbonyl carbon of cysteine. The latter cleavage could possibly arise by the loss of CO after cysteine-glycine peptide bond cleavage. The presence of these four ions indicates that the m/z 510 ion was produced by C5-C6 cleavage of the lipid backbone in precursor m/z 626. The mechanism for this cleavage process is similar to the one described by Griffiths et al. in negative ion experiments [14]. Cleavage of this bond would lead to a partial lipid backbone structure containing an allylic conjugated triene with the loss of neutral 5-oxo-pentanoic acid and cysteine-glycine-glutamate tripeptide unit attached via the sulfur atom.

In the MS² CID spectrum of LTC₄ (5, 6) isomer (Figure 2a), additional product ions appeared at m/z 233, 333, 351, 359, 376, 394, and 551 that were not previously reported in low-energy CID experiments. The low abundance fragments m/z 233 and 394 are the products of two bond cleavages that occur at facile sites. Possibly one of the bond cleavages is caused by CID and the other by a rearrangement process. Fragment m/z 233 was obtained by cleavage of the cysteine-glycine peptide bond and the C6-S thio-ether bond in the (5, 6) isomer. Ion m/z 394 was formed by breaking the cysteine-glutamate peptide bond and the bond between C α and carbonyl carbon of cysteine. Loss of water from 394 produces m/z 376. Ion m/z 551 was the product of glutamate loss from m/z 626. All of the above assignments were further supported by MS³ experiments (data not shown). Product ions at m/z 333, 351, and 359 were not sufficiently intense to perform MS³ CID experiments. However, they were successfully characterized by photodissociation, as discussed below. Most noteworthy, the fragmentation and rearrange-

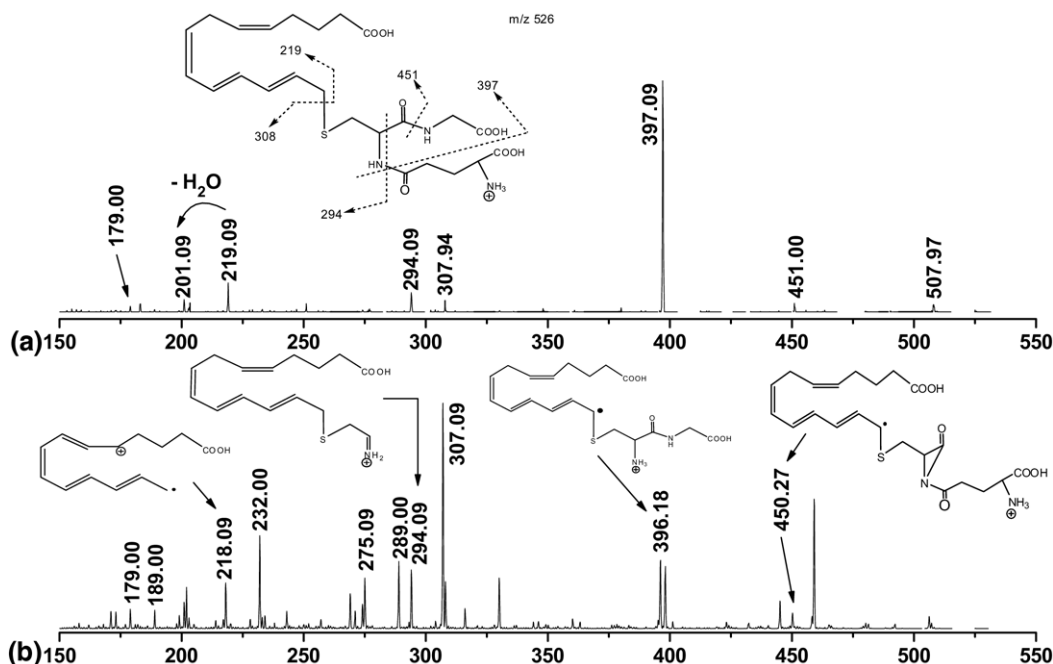


Figure 4. (a) MS³ CID spectrum of the fragment *m/z* 526 obtained from LTC₄ (14, 15) collisional activation, (b) MS³ CID spectrum of the photofragment *m/z* 525 obtained from LTC₄ (14, 15).

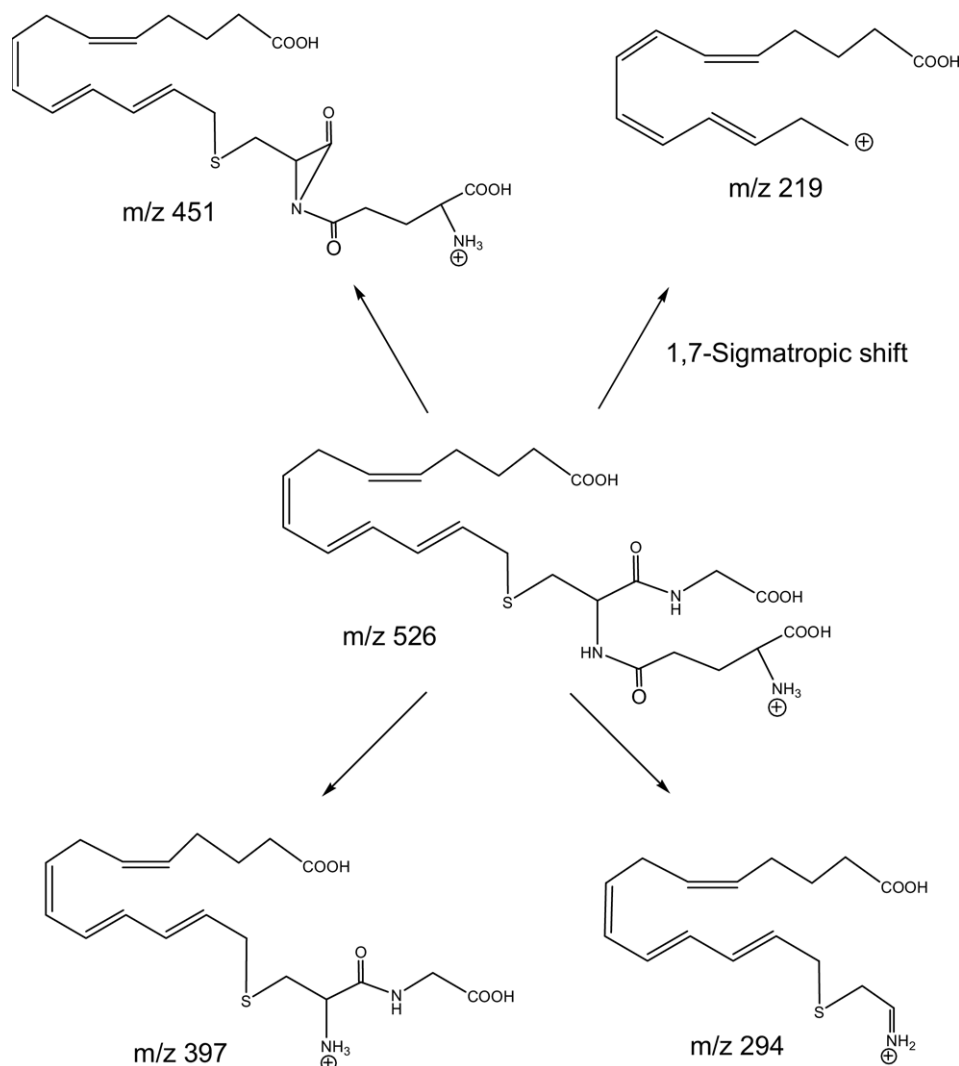
ment reactions observed in CID occurred via heterolytic bond cleavage processes.

The same LTC₄ (5, 6) molecule was subjected to 157 nm laser photofragmentation in the linear ion trap and the resulting spectrum is shown in Figure 2b. Although most of the product ions are similar to those in the low-energy CID spectrum, there are some significant differences. Most strikingly, there is a dramatic increase in the signals of characteristic features *m/z* 189 and 509. The product ion *m/z* 189 becomes the most intense peak in the spectrum, which suggests that the cleavage of the carbon-6 and carbon-7 of the lipid backbone is a prominent photochemical pathway following 157 nm excitation. The other valuable product ion, *m/z* 509, is 1 Da lighter than its CID counterpart and is dramatically enhanced by photofragmentation. A possible mechanism could be similar to the one discussed by Griffith et al. [14] We propose a direct photolysis of the C5–C6 bond on the lipid backbone that would form the ion *m/z* 509. To investigate this, we isolated the *m/z* 509 ion and fragmented it by CID. The hybrid MS³ spectrum is displayed in Figure 3b. A new product ion series *m/z* 189, 202, 232, 275, 289, 307, and 380 is generated that differs from the MS³ CID spectrum seen in Figure 3a. The proposed structures and the mechanisms of formation of these ions are depicted in Scheme 2a and b. It is interesting to note that the 232 and 307 *m/z* peaks are 1 Da lighter than their CID counterparts. They are apparently formed by homolytic radical cleavage of the C6–S bond adjacent to the photolysis site in the *m/z* 509 precursor ion. This would yield two radical products, one of which retains the charge proton. In the case of ion *m/z* 307, we believe the radical resides on sulfur

with the charge retained on one of the most basic nitrogens within the tripeptide unit. Subsequent cleavage of the cysteine-glycine peptide bond in *m/z* 307 could lead to the formation of *m/z* 232. On the other hand, heterolytic cleavage of the C6–S bond from *m/z* 509 and a subsequent rearrangement of the conjugated triene by a 1,8-sigmatropic shift would produce a resonance stabilized radical alkyl cation *m/z* 202. Scheme 2a displays the proposed mechanism for its formation. The presence of *m/z* 202, 232, 275, and 380 radical ions in the MS³ spectrum provides strong evidence for the radical ion structure of the *m/z* 509 fragment.

To further investigate the radical ion structure of *m/z* 307, we isolated and collisionally dissociated it in the trap. The resulting MS⁴ spectrum is presented in Figure 3c. Fragment ions *m/z* 178 and 232 provide important information about the radical structure of ion *m/z* 307 and the mechanism for their formation is illustrated in Scheme 2b. Sequential dehydration of *m/z* 307 leads to the other radical product ions *m/z* 289 and 271, respectively. Most of the MS⁴ fragments derived from ion *m/z* 307 were successfully assigned assuming a radical ion structure.

Close inspection of the MS² photodissociation spectrum (Figure 2b) revealed two additional diagnostic features for the (5, 6) isomer at *m/z* 381 and 465. They are only observable in the photofragmentation spectrum and their identities were also confirmed by hybrid MS³ (data not shown). These unique fragments are obtained by the losses of γ -glutamic acid and CO₂, respectively, from *m/z* 509 ion. They provide more evidence for the attachment of the tri-peptide unit at position C–6 of the lipid backbone that differentiates



Scheme 3. Proposed structures and pathways for production of some CID fragments.

LTC₄ (5, 6) from LTC₄ (14, 15). Other new findings are *m/z* 306, 434, 452, and 524 fragment ions, but they do not provide adequate information about the positional isomerism in the LTC₄ isomers. They are, however, helpful in providing additional information to support the lipid backbone structure in the precursor *m/z* 626. A double-bond formation between S-CH₂ of the cysteine side-chain during the C6-S bond cleavage process could lead to the formation of *m/z* 306 ion. Two proposed pathways for the formation of this ion are presented in Scheme 2c. Another interesting new feature at *m/z* 524 is the product of a homolytic bond cleavage between C α and the carbonyl carbon of cysteine. The fragment *m/z* 452 is attributable to a radical product ion produced by two bond cleavages within the tri-peptide unit. The combination of a homolytic cleavage between C α and COOH bond at the glycine terminus and a heterolytic cleavage at the cysteinyl-glutamate peptide bond leads to the formation of *m/z* 452. The weak ion at *m/z* 351 was formed by the scission of S-CH₂ bond with charge retention

on the lipid portion and the minor fragment *m/z* 359 corresponds to the loss of ammonia from *m/z* 376 ion. We also observe a doublet of peaks at *m/z* 581 and 582 in the photodissociation spectrum that corresponds to the loss of COOH radical (45 Da) and CO₂ (44 Da), respectively, from *m/z* 626 ion.

Protonated LTC₄ (14, 15) Isomer

Figure 2c shows a typical CID spectrum of singly charged protonated LTC₄ (14, 15) ion. Despite the apparent similarities with collisional activation spectrum of (5, 6) isomer, a few significant differences were observed. Unique features at *m/z* 205, 397, and 526 provide critical information about the linkage position of the tripeptide unit at carbon-14 of the lipid backbone via cysteinyl sulfur. Investigation of ion *m/z* 205 by MS³ CID revealed that the cleavage of C13-C14 lipid backbone in the molecule results in a resonance stabilized alkyl cation similar to the one discussed earlier for the (5, 6) isomer (data not

shown). Characteristic feature m/z 526 was produced by the scission of the C14–C15 bond on the lipid backbone in the m/z 626 ion. The structure of this ion is depicted in Table 1 and the corresponding MS³ spectrum is shown in Figure 4a with the inset illustrating internal fragments. Among them, only the diagnostic fragments at m/z 219, 294, 397, and 451 that help to characterize the ion m/z 526 and their structures are depicted in Scheme 3. The most intense feature m/z 397 involves the elimination of glutamate residue from m/z 526. Another minor product ion m/z 219 signifies the C14–S bond cleavage unique to the resonance stabilized alkyl cation. Also present in Figure 4a is the ion m/z 294 that defines the partial lipid backbone structure in m/z 526 and involves a rupture of two bonds across the tri-peptide unit.

The analogous ion-trap 157 nm photodissociation spectrum of LTC₄ (14, 15) isomer is presented in Figure 2d. What is particularly appealing in this spectrum is the abundance of characteristic features m/z 205 and 525 that enable the two isomers to be distinguished. The former is the most intense peak in the spectrum and it reveals that the carbon-13 and carbon-14 bond cleavage of the lipid chain is the predominant photochemical pathway during 157 nm light excitation. The m/z 525 photofragment ion is 1 Da lighter than its CID counterpart. This suggests that it is a radical ion. Direct photolysis of the C14–15 bond in the precursor molecule would lead to this radical product ion. To confirm this we collisionally dissociated m/z 525 ions in the ion trap. The resulting spectrum is displayed in Figure 4b. Ions at m/z 218, 294, 396, and 450 are new features that provide evidence for a radical ion structure of m/z 525. Heterolytic bond cleavage of the C14–S thioether bond followed by a 1,7-sigmatropic rearrangement of the conjugated triene would afford a resonance stabi-

lized radical alkyl cation m/z 218 as depicted in the spectrum inset. Cleavage of peptide bonds can generate m/z 396 and m/z 450 ions and provides additional evidence for radical ion structure. Notably, the abundance of the radical ion m/z 307 in this spectrum is analogous to our earlier CID results obtained from the photofragment m/z 509 of LTC₄ (5, 6) isomer (Figure 3b). Ion m/z 294 was formed by breaking the C α and carbonyl carbon bond in cysteine and the bond between cysteine–glutamate residues.

Thus far, we have compared the photofragmentation results with low-energy CID experiments. To investigate how photofragmentation compares with high-energy collisional activation, we analyzed the protonated LTC₄ (5, 6) and (14, 15) isomers in MALDI-TOF/TOF instrument using CHCA matrix, and the corresponding spectra are shown in Figure 5a and b. The resulting spectra of these isomers share some common features at m/z 308, 317, 331, 477, and 495, which are similar to our earlier low-energy CID and photofragmentation experiments. Features at m/z 415, 496, 532, 391, and 433 are unique to one isomer or the other. However, MS³ experiments to more thoroughly characterize these ions are not possible with the MALDI-TOF/TOF instrument. Unfortunately, important characteristic fragments such as m/z 510 for (5, 6) isomer and m/z 205 and 526 for (14, 15) isomer are missing from the spectra. The fragment information is significantly less than with other techniques. The poor S/N ratio can be associated with the inability of the mass spectrometer to isolate precursor ions within a 1 Da mass window. Also, MALDI ionization may not be as efficient as electrospray for these kinds of molecules and matrix clusters certainly contribute to spectral background [12, 13]. Thus, the information obtained from these fragments is not sufficient either to

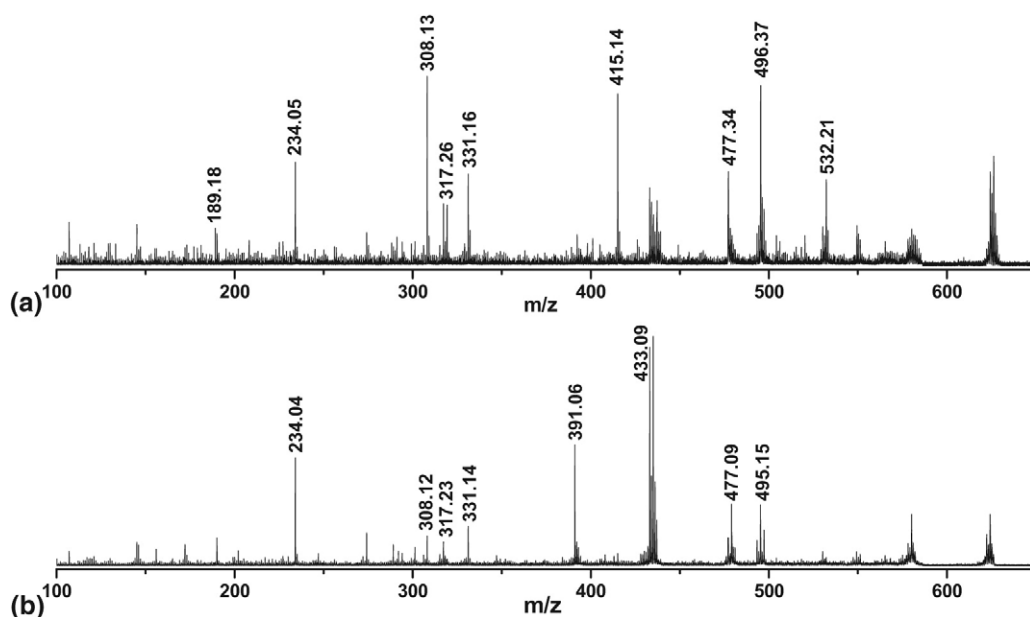


Figure 5. High-energy MS² CID spectrum of (a) [M + H]⁺ LTC₄ (5, 6) isomer, (b) [M + H]⁺ LTC₄ (14, 15) isomer.

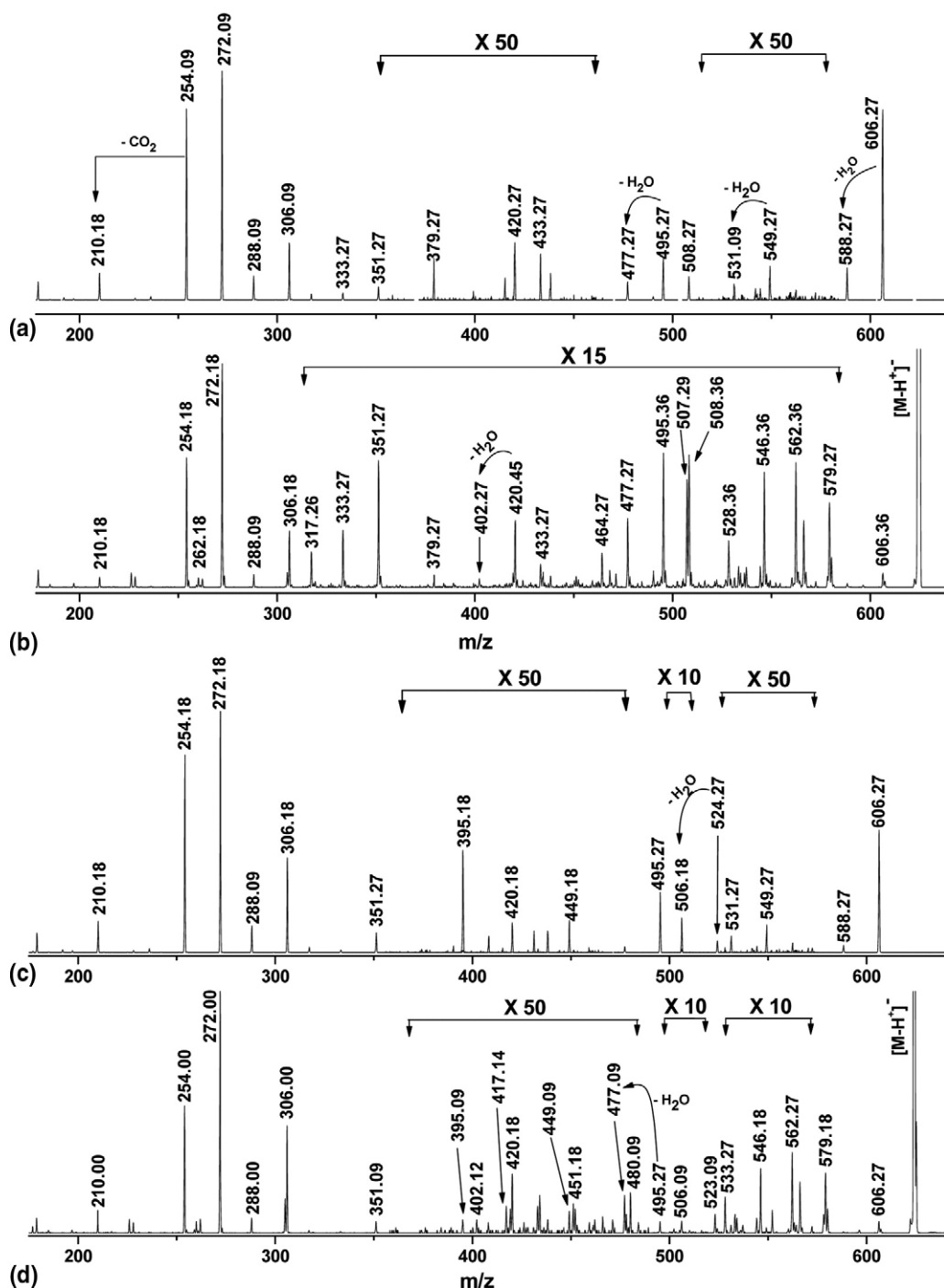


Figure 6. MS² spectra of [M - H]⁻ LTC₄ (5, 6) (precursor ion: *m/z* 624) obtained by (a) low-energy CID in linear ion trap, (b) 157 nm photodissociation in ion trap. MS² spectra of [M - H]⁻ LTC₄ (14, 15) obtained by (c) low-energy CID in ion trap, (d) 157 nm photodissociation in ion trap. Note changes in vertical scale within the spectrum.

identify or to distinguish the LTC₄ isomers. For this reason this technique was not pursued further in our work.

Negative Ion LTC₄

The cysteinyl leukotrienes produced abundant [M - H]⁻ ions following electrospray ionization due to the pres-

ence of free carboxylic acid moieties. It was of interest to learn how the negative charge affected the photofragmentation. Figure 6a and b show, respectively, the spectra obtained by CID and 157 nm light of the monoisotopically selected [M - H]⁻ LTC₄ (5, 6) isomer. The main spectral features correspond closely to those previously reported [14, 16, 25, 26]. However, it is

Table 2. Summary of characteristic product ions created in LTC₄ CID and 157 nm photofragmentation experiments

Type of precursor	LTC ₄ (5, 6)		LTC ₄ (14, 15)	
	CID	Photodissociation 157 nm	CID	Photodissociation 157 nm
[M + H] ⁺	189	189	205	205
	510	381	397	397
		465	526	525
		509		
[M – H] [–]	379	379	395	395
	508	464	449	449
		507	524	480
		508		523
[M + Na] ⁺	403	403	548	227
	532	531		547

pertinent here to emphasize that the formation of fragment ions m/z 464 and 507 was observed only in the photofragmentation spectrum and they help to distinguish the (5, 6) isomer from its counterpart. Ion m/z 464 was formed by the loss of CO₂ from m/z 508. The homolytic cleavage of the C5–C6 bond on the lipid backbone resulted in the formation of radical product ion m/z 507 as confirmed by MS³ experiments. This characteristic of the photofragmentation method has been observed for the (14, 15) isomer as well. Figure 6c and d show the CID and photodissociation spectra of LTC₄ (14, 15) isomer. The new feature at m/z 480 is only observable in the photofragmentation spectrum. The presence of this diagnostic ion was associated with CO₂ loss from ion m/z 524 and establishes the attachment position of the tripeptide unit to the C14 carbon of the lipid backbone. Although the m/z 524 ion is not seen in the photodissociation spectrum, the corresponding radical ion at m/z 523 is detected. It is formed by the direct photolysis of C14–C15 bond of the lipid chain and is unique to the photofragmentation spectrum. The structures of these fragments were proved by MS³ experiments (data not shown). Characteristic fragment ions that can distinguish the (5, 6) and (14, 15) isomers are summarized in Table 2. Although photofragmentation of [M – H][–] anions provided more informative fragment ions than CID, we found that the overall fragmentation efficiency of [M – H][–] anions using both techniques is significantly lower than with [M + H]⁺ ions. This behavior has been reported earlier by others following negative ion CID ion trap experiments [16]. The most intense feature observed in Figure 6 a–d is m/z 272, associated with the cleavage of C–S bond of the cysteine side chain with charge retention at the tripeptide unit. Thus, the major fragmentation channel is not significantly altered by photofragmentation.

Sodium Cationized LTC₄

Sodium cationized molecular ion species [M + Na]⁺ of LTC₄ isomers can be generated in abundance by an ESI source but have not been previously studied. To com-

pare the fragment ion distribution of [M + Na]⁺ to that of [M + H]⁺ and [M – H][–], we investigated the fragmentation behavior of [M + Na]⁺ from (5, 6) and (14, 15) isomers by CID and photofragmentation. Figure 7a and b were generated by CID and 157 nm light activation of the (5, 6) isomer. The observed product ion patterns are similar to those obtained by [M + H]⁺ and [M – H][–] species. Both spectra share the weak but characteristic feature at m/z 403 that helps to determine the tripeptide linkage site at the C5 position. Another diagnostic ion m/z 532 is also seen in the CID spectrum. Cleavage of the C5–C6 bond of the lipid chain resulted in the formation of m/z 532 and the subsequent elimination of γ -glutamate leads to ion m/z 403. Significantly, the radical fragment ion m/z 531 is unique to the photofragmentation spectrum. Other radical product ions such as m/z 297, 374, and 486 are also seen. MS³ experiments on these fragments revealed that a radical cleavage at S– β C bond of cysteine side chain in m/z 648 yields two radical ions. If the metal cation is retained on the tripeptide portion of the molecule, the resulting fragment ion mass is m/z 297. Alternatively, if it is retained by the lipid backbone, the product ion mass is m/z 374. Another radical ion m/z 486 is formed by the loss of –COOH from the photofragment m/z 531. The overall product ion abundance in the latter case is significantly stronger than CID. Since the structures of the other product ions in CID and photodissociation spectrum are familiar from our earlier discussion, further interpretation is not presented here.

Figure 7c and d show the result of CID and 157 nm activation of singly charged (14, 15) anions. The CID spectrum contains only one characteristic fragment ion at m/z 548 formed by the well known C14–C15 bond cleavage. By contrast, photofragmentation yielded diagnostic radical fragment ions such as m/z 227 and 547 (Table 2). Ion m/z 227 was obtained by C13–C14 bond cleavage of the lipid backbone.

Unfortunately, compared with [M + H]⁺ ion results, the lack of sufficient diagnostic product ions that permit the distinction between the isobaric structures is disappointing. Unlike [M + H]⁺ and [M – H][–] ions of LTC₄ isomers, the most intense peak at m/z 519 is associated with the cleavage of the cysteine–glutamate peptide bond. It appears to be the major fragmentation pathway observed in all of the above spectra (Figure 7a–d), which significantly limits the yield of other product ions. The differences in fragmentation induced by sodium-complexation with LTC₄ molecules are most likely due to the nature of metal coordination [27, 28]. While protonation is localized to the basic nitrogen atoms and deprotonation occurs at one of the three fixed carboxylic acid sites in the molecule, metals may undergo coordination with several oxygen atoms simultaneously. Such metal coordination could significantly affect the excitation process and thus the fragments generated.

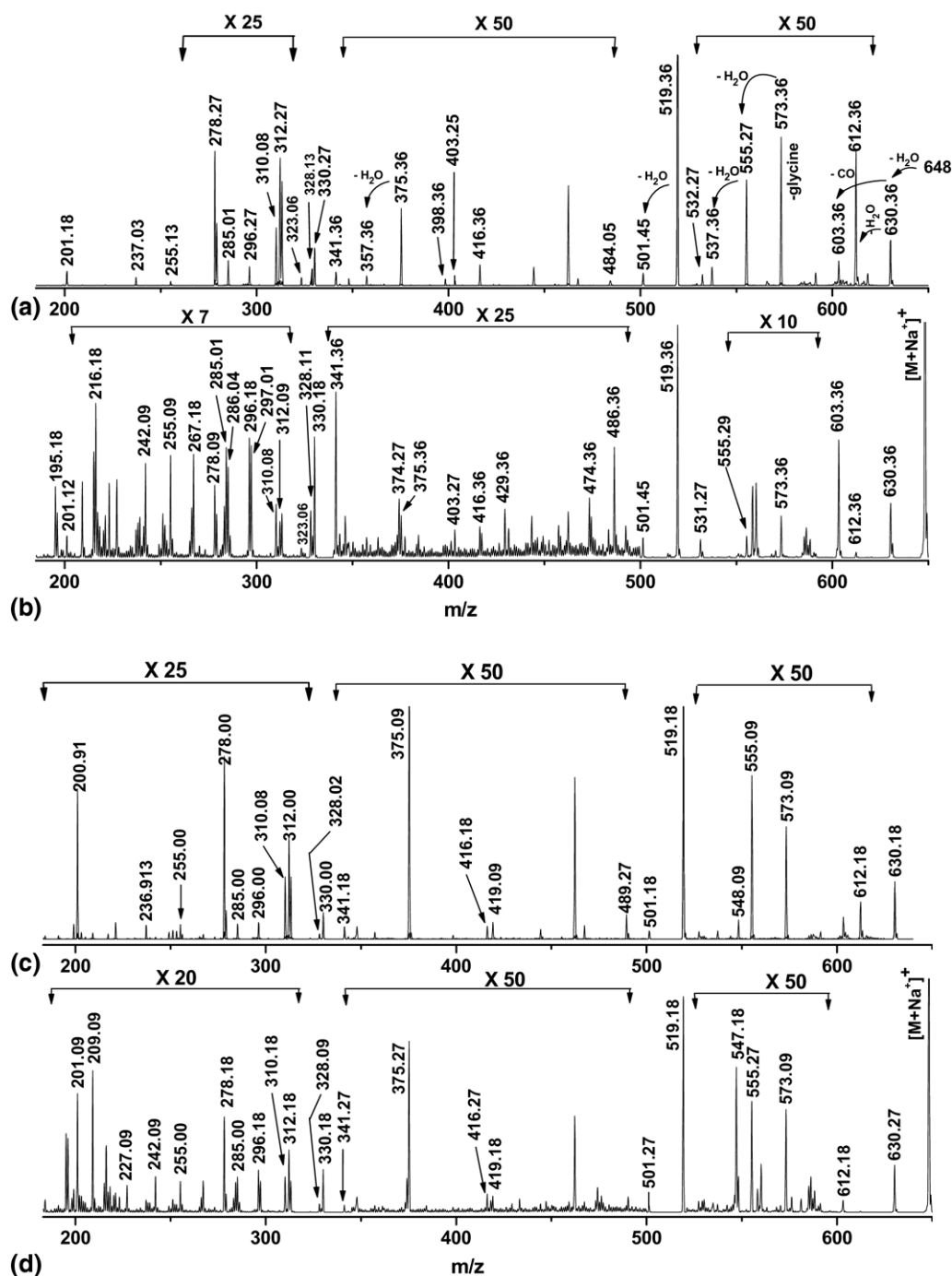


Figure 7. MS² spectra of [M + Na]⁺ LTC₄ (5, 6) (precursor ion: m/z 648) obtained by (a) low-energy CID in linear ion trap, (b) 157 nm photodissociation in ion trap. MS² spectra of [M + Na]⁺ LTC₄ (14, 15) obtained by (c) low-energy CID in ion trap, (d) 157 nm photodissociation in ion trap. Note changes in vertical scale within the spectrum.

Summary and Conclusions

[M + H]⁺, [M - H]⁻, and [M + Na]⁺ ions of LTC₄ (5, 6) and (14, 15) isomers were fragmented by 157 nm light and by CID in a linear ion trap mass spectrometer. The 157 nm photofragmentation of LTC₄ isomers generated characteristic radical fragment ions associated with homolytic bond cleavages that are not commonly observed in low-energy CID experiments. A significant

increase in the formation of diagnostic fragment ions that provide valuable information about the linkage positions of the isomers was observed. These ions may facilitate quantitative comparisons of the two isomers in biological systems.

The mechanisms presented by previous workers in this field provided valuable information in understanding the common fragmentation reactions of cysteinyl-

leukotrienes. Best results were obtained for singly-charged protonated LTC₄ isomers with 157 nm light activation. The product ion yield obtained either by CID or photofragmentation technique was noticeably lower for [M – H][–] and [M + Na]⁺ species than for [M + H]⁺ ions. Hybrid MSⁿ experiments involving the collisional dissociation confirmed the identities of diagnostic photofragments.

Acknowledgments

This work has been supported by the National Science Foundation grant no. CHE 0518324, CHE 0431991, and NIH/NCRR, National Center for Glycomics and Glycoproteomics (NCGG) grant no. RR018942.

References

- Samuelsson, B. An Elucidation of the Arachidonic Acid Cascade Discovery of Prostaglandins, Thromboxane, and Leukotrienes. *Drugs* **1987**, *33*, 2–9.
- Holtzman, M. J. Arachidonic Acid Metabolism. *Am. Rev. Respir. Dis.* **1991**, *143*, 188–203.
- Samuelsson, B.; Dahlen, S. E.; Lindgren, J. A.; Rouzer, C. A.; Serhan, C. N. Leukotrienes and Lipoxins: Structures, Biosynthesis, and Biological Effects. *Science* **1987**, *237*, 1171–1176.
- Smith, W. L.; Murphy, R. C. Prostaglandins and Leukotrienes. *Encycl. Biol. Chem.* **2004**, *3*, 452–456.
- Rokach, J. *Leukotrienes and Lipoygenases—Chemical, Biological, and Clinical Aspects*, Vol. II; Elsevier Publications: New York, 1989, p. 309.
- Murphy, R. C. Lipid Mediators, Leukotrienes, and Mass Spectrometry. *J. Mass Spectrom.* **1995**, *30*, 5–16.
- Capra, V.; Thompson, M. D.; Sala, A.; Cole, D. E.; Folco, G.; Rovati, G. E. Cysteinyl-Leukotrienes and Their Receptors in Asthma and Other Inflammatory Diseases: Critical Update and Emerging Trends. *Med. Res. Rev.* **2007**, *27*, 469–527.
- Samuelsson, B.; Hammarstrom, S. Leukotrienes: A Novel Group of Biologically Active Compounds. *Vitam. Horm.* **1982**, *39*, 1–30.
- Murphy, R. C.; Sala, A. *Treatise on Pulmonary toxicology: Comparative Biology of the Normal Lung*; CRC Press: New York, 1992; p 427.
- Piacentini, G. L.; Kaliner, M. A. The Potential Roles of Leukotrienes in Bronchial Asthma. *J. Am. Rev. Respir. Dis.* **1991**, *143*, S96–S99.
- Murphy, R. C.; Mathews, W. R.; Rokach, J.; Fenselau, C. Comparison of Biological-Derived and Synthetic Leukotriene C₄ by Fast Atom Bombardment Mass Spectrometry. *Prostaglandins* **1982**, *23*, 201–206.
- Keller, B. O.; Li, L. Discerning Matrix-Cluster Peaks in Matrix-Assisted Laser Desorption/Ionization Time-of-Flight Mass Spectra of Dilute Peptide Mixtures. *J. Am. Soc. Mass Spectrom.* **2000**, *11*, 88–93.
- Karthy, J. A.; Marcia, M. E.; Ireland, M. M. E.; Brun, Y. V.; Reilly, J. P. Artifacts and Unassigned Masses Encountered in Peptide Mass Mapping. *J. Chromatogr. B* **2002**, *782*, 363–383.
- Griffiths, W. J.; Yang, Y.; Sjoval, J.; Lindgren, J. A. Electrospray Tandem Mass Spectrometry of Cysteinyl Leukotrienes. *Rapid Commun. Mass Spectrom.* **1996**, *10*, 1054–1070.
- Murphy, R. C.; Barkley, R. M.; Berry, K. Z.; Hankin, J.; Harrison, K.; Johnson, C.; Krank, J.; McAnoy, A.; Uhlsou, C.; Zarini, S. Electrospray Ionization and Tandem Mass Spectrometry of Eicosanoids. *Anal. Biochem.* **2005**, *346*, 1–42.
- Hevko, J. M.; Murphy, R. C. Electrospray Ionization and Tandem Mass Spectrometry of Cysteinyl Eicosanoids; Leukotriene C₄ and FOG₇. *J. Am. Soc. Mass Spectrom.* **2001**, *12*, 763–771.
- Sailesh, S.; Kumar, Y. V. K.; Prasad, M.; Reddanna, P. Sheep Uterus Dual Lipoygenase in the Synthesis of 14, 15-Leukotrienes. *Arch. Biochem. Biophys.* **1994**, *315*, 362–368.
- Garcia, M.; Durand, T.; Rossi, J. C.; Zarini, S.; Bolla, M.; Folco, G.; Wheelan, P.; Sala, A. Synthesis and Biological Evaluation of 14, 15-Dehydro-LTA₄ analog. *Bioorg. Med. Chem. Lett.* **1997**, *7*, 105–108.
- Sala, A.; Garcia, M.; Zarini, S.; Rossi, J. C.; Folco, G.; Durand, T. 14, 15-Dehydroleukotriene A₄: A specific substrate for leukotriene C₄ synthase. *Biochem. J.* **1997**, *328*, 225–229.
- Thompson, M. S.; Cui, W.; Reilly, J. P. Fragmentation of Singly-Charged Peptides by Photodissociation at 157 nm. *Angew. Chem. Int. Ed.* **2004**, *43*, 4791–4794.
- Kim, T. K.; Thompson, M. S.; Reilly, J. P. Peptide Photodissociation at 157 nm in a Linear Ion Trap Mass Spectrometer. *Rapid Commun. Mass Spectrom.* **2005**, *19*, 1657–1665.
- Cui, W.; Thompson, M. S.; Reilly, J. P. Pathways of Peptide Ion Fragmentation Induced by Vacuum Ultraviolet Light. *J. Am. Soc. Mass Spectrom.* **2005**, *16*, 1384–1398.
- Devakumar, A.; Thompson, M. S.; Reilly, J. P. Fragmentation of Oligosaccharide Ions with 157 nm Vacuum Ultraviolet Light. *Rapid Commun. Mass Spectrom.* **2005**, *19*, 2313–2320.
- Devakumar, A.; Mechref, Y.; Kang, P.; Novotny, M. V.; Reilly, J. P. Laser-Induced Photofragmentation of Neutral and Acidic Glycans Inside an Ion-Trap Mass Spectrometer. *Rapid Commun. Mass Spectrom.* **2007**, *1452*–1460.
- Raftery, M. J.; Thorne, G. C.; Orkiszewski, R. S.; Gaskell, S. J. Preparation and Tandem Mass Spectrometric Analyses of Deuterium-Labeled Cysteine-Containing Leukotrienes. *Biomed. Environ. Mass Spectrom.* **1990**, *19*, 465–474.
- Sala, A.; Kayganich, K.; Zirrolli, J. A.; Murphy, R. C. Negative Ion Tandem Mass Spectrometry of Leukotriene E₄ and LTE₄ Metabolites: Identification of LTE₄ in Human Urine. *J. Am. Soc. Mass Spectrom.* **1991**, *2*, 314–321.
- Liu, H.; Hakansson, K. Electron Capture Dissociation of Tyrosine O-Sulfated Peptides Complexed with Divalent Metal Cations. *Anal. Chem.* **2006**, *8*, 7570–7576.
- Fung, Y. M.; Liu, H.; Chan, T. W. D. Electron Capture Dissociation of Peptides Metalated with Alkaline-Earth Metal Ions. *J. Am. Soc. Mass Spectrom.* **2006**, *17*, 757–771.